# Generating a Gaussian cosmological field for simulation of HERA observations: Notes and basic results

Zachary Martinot

Febuary 2018

## 1 The setup

We want to produce the visibilities that would be the result of observing a redshifted, Gaussian field with known power spectrum $P(k)$. The observed specific intensity $I$ in the direction $\hat{\mathbf{s}}$ at frequency $\nu$ is

$$I(\nu, \hat{\mathbf{s}}) = 2k_b \frac{\nu^2}{c^2} T(\nu, \hat{\mathbf{s}}) \text{ [Jy/sr]}. \tag{1}$$

The observed specific intensity $I(\nu)$ is related to the cosmological source specific intensity $I'(\nu')$ by invariance of the photon phase space number density, which produces

$$\frac{I(\nu)}{\nu^3} = \frac{I'(\nu')}{\nu'^3}. \tag{2}$$

In the rest frame of the source, $\nu' = \nu_e = 1420.4057\text{MHz}$, and the intensity of the emission is parameterized by a brightness temperature field $T(\vec{\mathbf{r}}, z)$. so that the brightness temperature of the observed redshifted radiation is then

$$\frac{T(\nu, \hat{\mathbf{s}})}{\nu} = \frac{T(\vec{\mathbf{r}}, z)\ \big|_{r=r_\nu, z=z_\nu}}{\nu_e} \tag{3}$$

where $z_\nu = \frac{\nu_e}{\nu} - 1$ is the redshift, $\vec{\mathbf{r}} = r\hat{\mathbf{s}}$ is the co-moving coordinate vector, and $r_\nu$ is the co-moving distance

$$r_\nu = r(\nu) = c \int_0^{z_\nu} \frac{\mathrm{d}z'}{H(z')}. \tag{4}$$

The cosmological brightness temperature field is further decomposed as

$$T(\vec{\mathbf{r}}, z) = \overline{T}(z) + \delta T(\vec{\mathbf{r}}, z) \tag{5}$$

$$= \overline{T}(z) + \int \frac{\mathrm{d}^3\vec{\mathbf{k}}}{(2\pi)^3} \delta\widetilde{T}(\vec{\mathbf{k}}, z) e^{i\vec{\mathbf{k}}\cdot\vec{\mathbf{r}}} \tag{6}$$

where $\delta\widetilde{T}$ is a Gaussian random field with

$$\left\langle \delta\widetilde{T}(\vec{\mathbf{k}}, z) \right\rangle = 0 \tag{7}$$

$$\left\langle \delta\widetilde{T}(\vec{\mathbf{k}}, z) \delta\widetilde{T}^*(\vec{\mathbf{k}}', z) \right\rangle = (2\pi)^3 P(k, z) \delta(\vec{\mathbf{k}} - \vec{\mathbf{k}}') \tag{8}$$

Alternatively, the field's statistics are characterized by the spatial covariance function

$$\xi(|\vec{\mathbf{r}}-\vec{\mathbf{r}}'|,z) = \langle \delta T(\vec{\mathbf{r}},z)\delta T(\vec{\mathbf{r}}',z)\rangle \tag{9}$$

$$= \frac{1}{2\pi^2}\int_0^\infty \mathrm{d}k\, k^2 j_0(|\vec{\mathbf{r}}-\vec{\mathbf{r}}'|k)P(k,z) \tag{10}$$

The observed $T(\nu,\hat{\mathbf{s}})$ is then a Gaussian field on the sphere for each $\nu$ with angular power spectrum

$$C_\ell(\nu) = \frac{2}{\pi}\int_0^\infty \mathrm{d}k\, k^2 (j_\ell(r_\nu k))^2 P(k,z_\nu) \tag{11}$$

The key feature of the redshifted 21cm emission is its frequency correlation structure, so what we actually need to fully specify the observed field is the cross-frequency angular power spectrum

$$\langle a_{\ell m}(\nu)a^*_{\ell' m'}(\nu')\rangle = C_\ell(\nu,\nu')\delta_{\ell\ell'}\delta_{mm'} \tag{12}$$

where

$$\delta T(\nu,\hat{\mathbf{s}}) = \sum_{\ell=0}^{\infty}\sum_{m=-\ell}^{\ell} a_{\ell m}(\nu)Y_{\ell m}(\hat{\mathbf{s}}). \tag{13}$$

Equivalently, the multi-frequency angular covariance function

$$\xi(\nu,\nu,\hat{\mathbf{s}}\cdot\hat{\mathbf{s}}') = \langle \delta T(\nu,\hat{\mathbf{s}})\delta T(\nu',\hat{\mathbf{s}}')\rangle \tag{14}$$

$$= \frac{1}{4\pi}\sum_{\ell=0}^{\infty}(2\ell+1)C_\ell(\nu,\nu')\mathcal{P}_\ell(\hat{\mathbf{s}}\cdot\hat{\mathbf{s}}'). \tag{15}$$

specifies the angular power spectrum by

$$C_\ell(\nu,\nu') = 4\pi\frac{1}{2}\int_{-1}^{1}\mathrm{d}\mu\,\mathcal{P}_\ell(\mu)\xi(\nu,\nu',\mu), \qquad \mu = \hat{\mathbf{s}}\cdot\hat{\mathbf{s}}'. \tag{16}$$

where $\mathcal{P}_\ell$ is the Legendre polynomial of order $\ell$.

Assume for now that the power spectrum is independent of redshift $P(k,z) = P(k)$. Then

$$C_\ell(\nu,\nu') = \frac{2}{\pi}\int_0^\infty \mathrm{d}k\, k^2 j_\ell(r_\nu k)j_\ell(r'_\nu k)P(k) \tag{17}$$

$$\xi(\nu,\nu',\mu) = \frac{1}{2\pi^2}\int_0^\infty \mathrm{d}k\, k^2 j_0(\gamma(\nu,\nu',\mu)k)P(k), \tag{18}$$

$$\gamma(\nu,\nu',\mu) = \sqrt{r_\nu^2 + r_\nu'^2 - 2r_\nu r'_\nu\mu} \tag{19}$$

## 1.1 Frequency discretization

We observe the sky in discrete frequency channels. The energy flux due to radiation incident from the direction $\hat{\mathbf{s}}$ in the frequency channel centered at $\nu_c$ with width $\Delta\nu$ is

$$\delta F(\nu_c, \Delta\nu, \hat{\mathbf{s}}) = \int_{\nu_c - \Delta\nu/2}^{\nu_c + \Delta\nu/2} \delta I(\nu, \hat{\mathbf{s}})\, \mathrm{d}\nu \tag{20}$$

$$= \frac{2k_b A_{Jy}}{c^2 \nu_e} \int_{\nu_c - \Delta\nu/2}^{\nu_c + \Delta\nu/2} \nu^3 \delta T(\nu, \hat{\mathbf{s}})\, \mathrm{d}\nu \, [\text{Jy Hz / sr}], \qquad A_{Jy} = 10^{26} \text{Jy } /(\text{W/m}^2/\text{Hz}). \tag{21}$$

On the other hand, visibilities tend to be interpreted as measurements in Jy, i.e. have units of flux spectral density, which allows the value to be equivalently described by a brightness temperature. This effectively refers to an average specific intensity on the sky in the frequency channel $\nu_c$

$$\delta \overline{I}(\nu_c, \hat{\mathbf{s}}) = \frac{1}{\Delta\nu} \delta F(\nu_c, \hat{\mathbf{s}}) \tag{22}$$

$$= \frac{2k_b A_{Jy}}{c^2 \nu_e} \frac{1}{\Delta\nu} \int_{\nu_c - \Delta\nu/2}^{\nu_c + \Delta\nu/2} \nu^3 \delta T(\nu, \hat{\mathbf{s}})\, \mathrm{d}\nu \, [\text{Jy / sr}]. \tag{23}$$

For our purposes the channel width is the same $\Delta\nu$ for all $\nu_c$ so we drop the explicit functional dependence, but of course it could vary in general. The angular covariance function of the average specific intensity of the cosmological field is then

$$\overline{\xi}(\nu_c, \nu'_c, \mu) = \left\langle \delta \overline{I}(\nu_c, \hat{\mathbf{s}}) \delta \overline{I}(\nu'_c, \hat{\mathbf{s}}') \right\rangle \tag{24}$$

$$= \left( \frac{2k_b A_{Jy}}{c^2 \nu_e} \right)^2 \frac{1}{\Delta\nu^2} \int_{\nu_c - \Delta\nu/2}^{\nu_c + \Delta\nu/2} \int_{\nu'_c - \Delta\nu/2}^{\nu'_c + \Delta\nu/2} \mathrm{d}\nu\, \mathrm{d}\nu'\, \nu^3 \nu'^3 \xi(\nu, \nu', \mu) \tag{25}$$

The cross-frequency angular power spectrum of the discretized observed specific intensity is then

$$\overline{C}_\ell(\nu_c, \nu'_c) = 2\pi \int_{-1}^{1} \mathrm{d}\mu\, \overline{\xi}(\nu_c, \nu'_c, \mu) \mathcal{P}_\ell(\mu) \ [\text{Jy}^2/\text{sr}^2]. \tag{26}$$

# 2 A simple (but not too simple) power spectrum

## 2.1 Power spectrum terms

We choose a power spectrum with terms of the form

$$P(k) \sim k^{\alpha - 1} e^{-\beta k} \tag{27}$$

as the normalization and the correlation function can be computed analytically. When normalized, this is also a pdf known as the gamma distribution, presumably because it is additionally the integrand for the definition of the gamma function. For our purposes it seems more appropriate to choose a factor that gives a unit total variance:

$$1 = \frac{A}{2\pi^2}\int_0^\infty \mathrm{d}k\, k^2 k^{\alpha-1} e^{-\beta k} \tag{28}$$

$$= \frac{A}{2\pi^2}\frac{\Gamma(\alpha+2)}{\beta^{\alpha+2}} \tag{29}$$

$$\implies P(k) = \frac{2\pi^2\beta^{\alpha+2}}{\Gamma(\alpha+2)} k^{\alpha-1} e^{-\beta k} \tag{30}$$

## 2.2 Angular Covariance

The angular covariance function for this power spectrum is

$$\xi(\gamma) = \frac{1}{2\pi^2}\int_0^\infty \mathrm{d}k\, k^2 j_0(\gamma k) P(k) \tag{31}$$

$$= \frac{\beta^{\alpha+2}}{\Gamma(\alpha+2)}\int_0^\infty \mathrm{d}k\, k^2 \frac{\sin(\gamma k)}{\gamma k} k^{\alpha-1} e^{-\beta k} \tag{32}$$

$$= \frac{\beta^{\alpha+2}}{\Gamma(\alpha+2)\gamma}\int_0^\infty \mathrm{d}k\, k^\alpha e^{-\beta k}\sin(\gamma k). \tag{33}$$

Noting that

$$\int_0^\infty \mathrm{d}k\, k^\alpha e^{-\beta k}\sin(\gamma k) = \mathrm{Im}\left\{\int_0^\infty \mathrm{d}k\, k^\alpha e^{-\beta k} e^{i\gamma k}\right\} \tag{34}$$

the integral is given by the Laplace transform of $k^\alpha$ evaluated at $\beta - i\gamma$,

$$\int_0^\infty \mathrm{d}k\, k^\alpha e^{-(\beta - i\gamma)k} = \frac{\Gamma(\alpha+1)}{(\beta - i\gamma)^{\alpha+1}} \tag{35}$$

$$= \Gamma(\alpha+1)\left(\frac{1}{\sqrt{\beta^2+\gamma^2}}\right)^{\alpha+1} e^{i(\alpha+1)\,\mathrm{atan}\left(\frac{\gamma}{\beta}\right)} \tag{36}$$

The covariance function is thus

$$\xi(\gamma) = \frac{\Gamma(\alpha+1)\beta^{\alpha+2}}{\Gamma(\alpha+2)\gamma}\left(\frac{1}{\sqrt{\beta^2+\gamma^2}}\right)^{\alpha+1}\sin\left((\alpha+1)\,\mathrm{atan}\left(\frac{\gamma}{\beta}\right)\right) \tag{37}$$

It can be useful to re-parameterize this expression by defining

$$\tan(\varphi) = \frac{\gamma}{\beta},\ (\text{note that } \gamma \geq 0,\ \beta > 0) \tag{38}$$

$$\cos(\varphi) = \frac{\beta}{\sqrt{\beta^2+\gamma^2}}. \tag{39}$$

Then,

$$\xi(\varphi) = \frac{\beta}{\alpha+1}\frac{\cos(\varphi)}{\beta\sin(\varphi)}\cos^{\alpha+1}(\varphi)\sin((\alpha+1)\varphi) \tag{40}$$

$$= \frac{1}{\alpha+1}\cos^{\alpha+2}(\varphi)\frac{\sin((\alpha+1)\varphi)}{\sin(\varphi)}, \tag{41}$$

$$\varphi(\nu,\nu',\mu) = \operatorname{atan}\left(\frac{\sqrt{r(\nu)^2+r(\nu')^2-2r(\nu)r(\nu')\mu}}{\beta}\right) \tag{42}$$

For evaluating this function at small values of $\varphi$ (corresponding to small $\gamma$ near $(\nu,\nu',\mu) = (\nu,\nu,1)$), the series expansion of the last factor is

$$\frac{\sin((\alpha+1)\varphi)}{\sin(\varphi)} = \alpha+1-\varphi^2\left(\frac{\alpha^3}{6}+\frac{\alpha^2}{2}+\frac{\alpha}{3}\right)+\mathcal{O}(\varphi^4) \tag{43}$$

## 2.3 Multiple components

To produce a variety of functional forms we can define the power spectrum as a sum of $N$ components

$$P(k) = \frac{2\pi^2\sigma^2}{\sum_{i=0}^{N-1} a_i}\sum_{i=0}^{N-1} a_i \frac{\beta_i^{\alpha_i+2}}{\Gamma(\alpha_i+2)}k^{\alpha_i-1}e^{-\beta_i k}. \tag{44}$$

The normalized weighting of the terms of unit variance means that the total variance/overall amplitude is set by $\sigma^2$. The angular covariance function is then

$$\xi(\nu,\nu',\mu) = \frac{\sigma^2}{\sum_{i=0}^{N-1} a_i}\sum_{i=0}^{N-1} a_i\xi_i(\varphi_i) \tag{45}$$

$$= \frac{\sigma^2}{\sum_{i=0}^{N-1} a_i}\sum_{i=0}^{N-1}\frac{a_i}{\alpha_i+1}\cos^{\alpha_i+2}(\varphi_i)\frac{\sin((\alpha_i+1)\varphi_i)}{\sin(\varphi_i)} \tag{46}$$

## 2.4 A fiducial power spectrum

An example two component power spectrum with parameters

$$\sigma^2 = 10^{-6}\ \mathrm{K}^2 \tag{47}$$

$$a_1 = 1 \tag{48}$$

$$a_2 = 10 \tag{49}$$

$$\alpha_1 = 7 \tag{50}$$

$$\alpha_2 = 20 \tag{51}$$

$$\beta_1 = 100\ \mathrm{Mpc}/h \tag{52}$$

$$\beta_2 = \frac{100}{3}\ \mathrm{Mpc}/h. \tag{53}$$

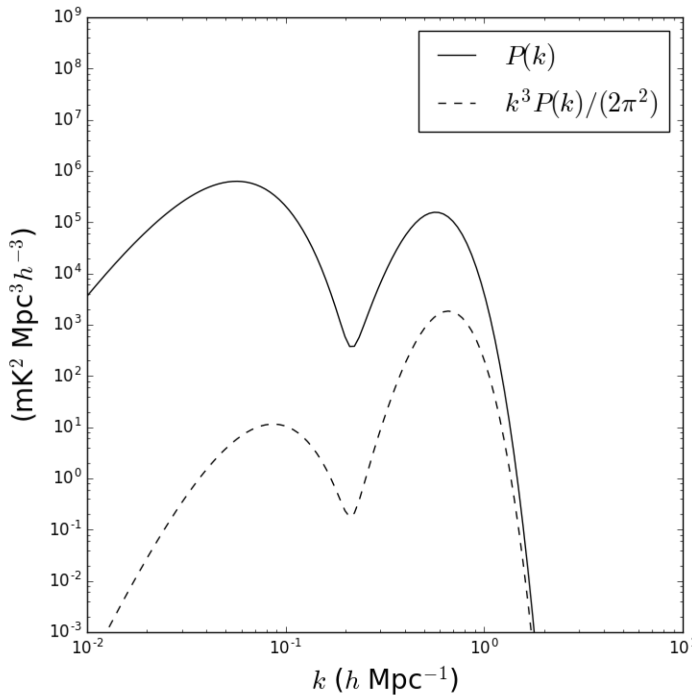


Figure 1: The power spectrum defined by these parameters.

# 3 Numerical Integration considerations

The numerical integration of Equation 16 to obtain the cross-frequency angular power spectrum is performed with `scipy.integrate.quad`, which is a wrapper for the Fortran subroutine package QUADPACK. In addition a fixed precision Gaussian quadrature can be used in principle.

The reference for the techniques and algorithms implemented in QUADPACK is "Quadpack, A Subroutine Package for Automatic Integration", by R. Piessens, D.K. Kahaner, E. de Doncker-Kapenga, C.W. Überhuber. The `scipy` documentation is rather limited. To discover how the inputs to the `quad` function map to the QUADPACK algorithms it is necessary to inspect the `scipy.integrate` code.

Three integration algorithms were implemented and compared in brief tests, and though the testing was in no way exhaustive, it appears that the QAWO algorithm is the most efficient of the three for this problem. Compared to the other QUADPACK algorithm applicable to this problem (QAGP) it also requires less analysis of the integrand, which I hope will make it more stable in general, although after some analysis the QAGS version was also entirely stable in the tests performed, it was just slower than than the QAWO version. Over most of the parameters space the two methods gave identical answers to within the specified tolerance, the only notable difference was that the QAWO algorithm managed to maintain accuracy for slightly smaller values of the integral.

The fixed-point Gaussian method was added because it is a nice additional check, as it ended up being simple to code, and has nice theoretical properties. But, it turns out to be rather inefficient compared to the automatic integration routines, producing significantly less precise results in significantly longer run times for the same integrations (for a clear reason, see section below). It did converge to the same answer as the other two method, which lends additional confidence to the results.

The frequency discretization integrals are much less demanding than those of Equation 16 and thus can be done relatively quickly with high precision using a fixed low order Gaussian rule.

## 3.1 Quadrature for the frequency channelization integrals

For reasonable parameter sets $(\vec{\mathbf{a}}, \vec{\boldsymbol{\alpha}}, \vec{\boldsymbol{\beta}})$ the function $\xi(\nu, \nu', \mu)$ is quite smooth in $\nu, \nu'$ over frequency channels of width $\sim 0.1$MHz and so the integrals in frequency can be computed very precisely with a fixed low-order Gaussian quadrature rule. In particular, for the fiducial power spectrum shown in another section, a 5-point rule appears sufficient to compute the channelization integrals for all channels of width $\sim 0.1$MHz between 100MHz and 200MHz. On the other hand, it may be the case that this integration causes unnecessary complications, and we could instead decide to pretend that our frequency channels are much narrower than the difference between channel center, and simply sample the integrand at those channel centers, i.e. set $\overline{C}_\ell(\nu, \nu') \propto C_\ell(\nu, \nu')$(with the unit conversion factor). This speeds the computation, and may make the result easier to use in testing.

## 3.2 Quadrature using the QAGP routine in QUADPACK (through scipy.integrate.quad)

Generally, calling the `quad` function will route to the QAGS routine. A naive application of `quad` to Equation 16 with the minimum required input yields useless results. The tolerances `epsabs` and `epsrel`, defined in the QUADPACK text, need to be set with some consideration of the range of values of the integral. The default `epsabs` will tend to prevent proper convergence when the integrand is small compared to 1. In addition, the integrand in this problem is both highly oscillatory ($\mathcal{P}_\ell$) and sharply peaked ($\xi$). It is thus necessary to provide a set of end points within the integration domain $\mu \in [-1, 1]$ between which the function does not vary so significantly. This will cause a different QUADPACK algorithm, QAGP, to be used. We can choose our break points by computing approximately the zeros $\{z_{\ell,n}\}_{n=1}^{\ell}$ of the Legendre polynomial of order $\ell$, given by

$$z_{\ell,n} \approx \left(1 - \frac{1}{8\ell^2} + \frac{1}{8\ell^3}\right) \cos\left(\pi \frac{4n-1}{4\ell+2}\right) \tag{54}$$

This formula may not be accurate enough for use in a Gaussian quadrature rule, but it is more than sufficient for breaking up the integral into segments with sufficiently constrained total variation that each segment can be handled easily by the automatic integration algorithm.

In addition, the angular covariance $\xi$ is often effectively zero over some significant part of the interval $\mu \in [-1, 1]$, i.e

$$\left| \int_{-1}^{\mu_c} \overline{\xi}(\nu, \nu', \mu) \mathcal{P}_\ell(\mu) \, \mathrm{d}\mu \right| \leq \int_{-1}^{\mu_c} \left| \overline{\xi}(\nu, \nu', \mu) \right| \mathrm{d}\mu = f(\mu_c) \approxeq 0, \text{ for some } \mu_c \in [-1, 1] \tag{55}$$

Such a point can be found by a numerical root finder applied to a function $g(\mu) = f(\mu) - \epsilon$, where $f(\mu)$ is the integral about evaluated numerically and $\epsilon$ is a threshold below which this tail of the integral can be ignored. The provided break points can then be limited to $z_{\ell,n} > \mu_c$ to avoid forcing the algorithm to spend a lot of time computing approximation of zero on the region $[-1, \mu_c]$.

With break points provided in this manner the result seems to be stable over the $(\ell, \nu, \nu')$ domain and achieves the precision requested by the `epsrel` parameter. However, it seems to be slower than the QAWO algorithm.

The QAGS/QAGP routines use a 21 point Gauss-Kronrod integration rule.

### 3.3 Quadrature for the angular integral using the QAWO routine in QUADPACK (through scipy.integrate.quad)

We can transform the integral to be computed (Equation 16) with a change of variables $\mu = \cos(\theta)$ so that

$$\overline{C}_\ell(\nu, \nu') = 2\pi \int_0^\pi \mathrm{d}\theta \sin(\theta) \mathcal{P}_\ell(\cos(\theta)) \overline{\xi}(\nu, \nu', \cos(\theta)) \tag{56}$$

This allows the use of the QAWO algorithm which integrates an arbitrary function $f(x)$ against a $\cos(\omega x)$ or $\sin(\omega x)$ weight function over a finite interval, for a specified real-valued $\omega$. In our case we choose the `'sin'` weight and $\omega = 1$. This algorithm is based on modified Clenshaw-Curtis quadrature, though it apparently also uses a 10 point Gauss-Kronrod rule in some situations. The QAWO routine does not use a set of break points. If `quad` is called with both the break points option and the weight function option set at the same time, the QAWO routine will be used and the break points will be unused.

### 3.4 Quadrature using a fixed precision Gaussian rule

The Gaussian quadrature rule of order $n$ for the average value of a function $f(\nu)$ on an interval $[a, b]$ is

$$\frac{1}{b-a} \int_a^b f(\nu) \, \mathrm{d}\nu \approx \frac{1}{2} \sum_{i=1}^{n} w_i f\left( \frac{b-a}{2} x_i + \frac{a+b}{2} \right) \tag{57}$$

where the nodes $\{x_i\}_{i=1}^n \subset [-1, 1]$ are the roots of the Legendre polynomial $\mathcal{P}_n(x)$ and the weights $w_i$ are

$$w_i = \frac{2}{(1 - x_i^2)(\mathcal{P}'_n(x_i))^2} \tag{58}$$

These nodes and weights are computed by the function `scipy.special.roots_legendre`. A low-order rule of this form is used to compute the integrals in Equation 25.

It is possible in principle to use such a rule to compute Equation 16, but the order of the rule must be large enough that $C_\ell \approx 0$ for $\ell > n$. The $C_\ell$ do eventually tend steeply to zero for this class of $P(k)$, but an estimate of when this occurs must be known to choose an appropriately large $n$. For reference, the fiducial power spectrum shown in the previous section, the angular power spectrum has its second peak at $\ell < 10^4$. A rule of order $n = 2 \times 10^4$ produced effectively the same result as both the QAGP and QAWO methods, but with a significant bias compared to the precision of `epsrel`$= 10^{-10}$ set in the two automatic routines (which agreed with each other to within this tolerance), and with a run time a factor of ∼2-5 larger than the QAGP method. In this case the order of the rule was chosen based on observing when the $C_\ell$ as previously computed by the other methods became small. In principle it should be possible to estimate this based on the parameters of $P(k)$ and the integral of Equation 17.

### 3.5 An idea for using DFTs

This section is only speculative. It seems that a custom quadrature method could be implemented using FFT's, which could produce an efficient method. The Legendre polynomial $\mathcal{P}_\ell(\cos(\theta))$ has a finite Fourier series for each $\ell$,

$$\mathcal{P}_\ell(\cos(\theta)) = \sum_{-\ell}^{-\ell} p_{\ell,n} e^{in\theta}. \tag{59}$$

Since $\xi(\cos(\theta))$ is very smooth at $\theta = 0$ (i.e.$\mu = 1$), and if it is not entirely flat at $\theta = \pi$ it is getting close, we can make a periodic extension of $\xi$ to the interval $[-\pi, \pi]$ to produce a function $\tilde{\xi}$ which is periodic, $\tilde{\xi}(\theta) = \tilde{\xi}(\theta + 2\pi)$ and continuous at $\theta = 0, \theta = \pi$, the boundary of the original domain. The Fourier series of the periodic extension

$$\tilde{\xi}(\cos(\theta)) = \sum_{m=-\infty}^{\infty} \tilde{\xi}_m e^{im\theta} \tag{60}$$

may then be fairly compact, in the sense that the coefficients $\tilde{\xi}_m$ are small enough to be ignored for some sufficiently large $m$. The Fourier coefficients may then be computed by FFT. The question is how large an $M$ is needed to provide a sufficient estimate of the integral as

$$\pi \int_{-\pi}^{\pi} \mathrm{d}\theta \sin(\theta) \mathcal{P}_\ell(\cos(\theta)) \tilde{\xi}(\cos(\theta)) \approx \sum_{m=-M}^{M} \sum_{n=-\ell}^{\ell} \tilde{\xi}_m p^*_{\ell,n} \pi \int_{-\pi}^{\pi} \mathrm{d}\theta \sin(\theta) e^{i\theta(n-m)} \tag{61}$$

and then additionally how large an FFT is need to accurately enough estimate the Fourier coefficients of $\tilde{\xi}$ up to that $M$. An interesting analysis of this issue is C.L. Epstein 2005, "How well does the finite Fourier transform approximate the Fourier transform?".

It then remains to be seen if in the end the whole scheme including computing the sum is actually more efficient than the automatic integration methods.

This is essentially Clenshaw-Curtis quadrature, at least in spirit if not definition, applied using additional specific knowledge of the integrand. It is also, I think, a recapitulation of a more specific case of the spherical harmonic transform described in McEwen 2011.

# 4 Other Useful Analytic Results

## 4.1 A "White Noise" Power Spectrum

If the cosmological field has equal power at all scales the power spectrum is

$$P(k) = P_0 = \text{ constant} \tag{62}$$

and cross-frequency angular power spectrum is

$$C_\ell(\nu, \nu') = \frac{2}{\pi}\int_0^\infty \mathrm{d}k\, k^2 j_\ell(r_\nu k) j_\ell(r'_\nu k) P(k) \tag{63}$$

$$= \frac{2P_0}{\pi}\int_0^\infty \mathrm{d}k\, k^2 j_\ell(r_\nu k) j_\ell(r'_\nu k) \tag{64}$$

$$= \frac{2P_0}{\pi}\frac{\pi}{2r_\nu r'_\nu}\delta(r_\nu - r'_\nu) \tag{65}$$

Note the units here are indeed $\mathsf{Temperature}^2$. The delta function simplifies with the multi-dimensional generalization of the function composition identity

$$\delta(g(\vec{\mathbf{s}})) = \int_{\mathcal{S}} \mathrm{d}\vec{\mathbf{a}}\, \frac{\delta(\vec{\mathbf{s}} - \vec{\mathbf{a}})}{|\boldsymbol{\nabla} g(\vec{\mathbf{a}})|}, \text{ where } \mathcal{S} = \{\vec{\mathbf{a}} : g(\vec{\mathbf{a}}) = 0\}. \tag{66}$$

Let $(\nu, \nu') = \vec{\mathbf{s}}$ and $g(\vec{\mathbf{s}}) = g(\nu, \nu') = r(\nu) - r(\nu')$. Then

$$\delta(r(\nu) - r(\nu')) = \int_0^\infty \mathrm{d}a\, \sqrt{2}\frac{\delta(\nu - a)\delta(\nu' - a)}{\sqrt{\left(\frac{\mathrm{d}r(\nu)}{\mathrm{d}\nu}\right)^2 + \left(\frac{\mathrm{d}r(\nu')}{\mathrm{d}\nu'}\right)^2}} \tag{67}$$

$$= \frac{1}{\left|\frac{\mathrm{d}r(\nu)}{\mathrm{d}\nu}\right|}\delta(\nu - \nu') \tag{68}$$

The factor of $\sqrt{2}$ in the first line is due to the integral being along the ray $\nu = \nu'$ in the $(\nu, \nu')$ plane. Thus

$$C_\ell(\nu, \nu') = \frac{P_0}{r_\nu r'_\nu \left|\frac{\mathrm{d}r(\nu)}{\mathrm{d}\nu}\right|}\delta(\nu - \nu') \tag{69}$$

We can check that the angular correlation function is then

$$\xi(\nu, \nu', \hat{\mathbf{s}}\cdot\hat{\mathbf{s}}') = \frac{1}{4\pi}\sum_{\ell=0}^{\infty}(2\ell+1)C_\ell(\nu, \nu')\mathcal{P}_\ell(\hat{\mathbf{s}}\cdot\hat{\mathbf{s}}') \tag{70}$$

$$= \frac{P_0}{r_\nu r'_\nu \left|\frac{\mathrm{d}r(\nu)}{\mathrm{d}\nu}\right|}\delta(\nu - \nu')\sum_{\ell=0}^{\infty}\frac{(2\ell+1)}{4\pi}\mathcal{P}_\ell(\hat{\mathbf{s}}\cdot\hat{\mathbf{s}}') \tag{71}$$

$$= \frac{P_0}{r_\nu r'_\nu \left|\frac{\mathrm{d}r(\nu)}{\mathrm{d}\nu}\right|}\delta(\nu - \nu')\delta(1 - \hat{\mathbf{s}}\cdot\hat{\mathbf{s}}') \tag{72}$$

as it should be. Assuming a set of disjoint equal-width frequency channels $\nu_c$, the averaged cross-frequency angular power spectrum is

$$\overline{C}_\ell(\nu_c, \nu_c') = \left(\frac{2k_b A_{Jy}}{c^2 \nu_e}\right)^2 \frac{1}{\Delta\nu^2} \int_{\nu_c - \Delta\nu/2}^{\nu_c + \Delta\nu/2} \int_{\nu_c' - \Delta\nu/2}^{\nu_c' + \Delta\nu/2} \mathrm{d}\nu \, \mathrm{d}\nu' \, \nu^3 \nu'^3 C_\ell(\nu, \nu') \tag{73}$$

$$= \delta_{\nu_c, \nu_c'} \left(\frac{2k_b A_{Jy}}{c^2 \nu_e}\right)^2 \frac{P_0}{\Delta\nu^2} \int_{\nu_c - \Delta\nu/2}^{\nu_c + \Delta\nu/2} \mathrm{d}\nu \, \frac{\nu^6}{r(\nu)^2 \left|\frac{\mathrm{d}r(\nu)}{\mathrm{d}\nu}\right|} \tag{74}$$

## 4.2 A Power-law

If the power spectrum takes the form

$$P(k) = A_0 k^{-2} \tag{75}$$

then the angular covariance function is

$$\xi(\nu, \nu', \mu) = \frac{1}{2\pi^2} \int_0^\infty \mathrm{d}k \, k^2 \frac{\sin(\gamma k)}{\gamma k} A_0 k^{-2}. \tag{76}$$

From the identity $\int_0^\infty \frac{\sin(x)}{x} = \frac{\pi}{2}$, we thus have

$$\xi(\nu, \nu', \mu) = \frac{A_0}{4\pi\gamma} \tag{77}$$

$$= \frac{A_0}{4\pi} \frac{1}{\sqrt{r_\nu^2 + r_\nu'^2 - 2 r_\nu r_\nu' \mu}} \tag{78}$$

$$= \frac{A_0}{4\pi} \sum_{\ell=0}^\infty \frac{r_\nu'^\ell}{r_\nu^{\ell+1}} \mathcal{P}_\ell(\mu), \text{ for } r_\nu' < r_\nu \tag{79}$$

Then the multi-frequency angular power spectrum is

$$C_\ell(\nu, \nu') = 2\pi \int_{-1}^1 \mathrm{d}\mu \, \mathcal{P}_\ell(\mu) \frac{A_0}{4\pi} \sum_{\ell'=0}^\infty \frac{r_\nu'^{\ell'}}{r_\nu^{\ell'+1}} \mathcal{P}_{\ell'}(\mu) \tag{80}$$

$$= \frac{A_0}{2\ell + 1} \frac{r_\nu'^\ell}{r_\nu^{\ell+1}}, \text{ for } r_\nu' < r_\nu. \tag{81}$$

# 5 An unphysical feature of these Gaussian brightness fields

It is worth noting that the brightness $I(\nu, \hat{\mathbf{s}}) = \overline{I}(\nu) + \delta I(\nu, \hat{\mathbf{s}})$ generated as a realization of a Gaussian random field is generally unphysical since it can take negative values. That is, any particular realization can potentially have $-\delta I(\nu, \hat{\mathbf{s}}) > \overline{I}(\nu)$ for some $(\nu, \hat{\mathbf{s}})$, though this may be made a rare occurrence by making the mean large compared to the variance. However, this is fine for use in the intended application of testing a power spectrum estimator. Although we know that the visibilities are sourced by a positive-definite field on the sky, this fact does not inform the power spectrum estimators. In other words, the same estimator is just as valid for a hypothetical measurement which is described by exactly the same formalism and in which the field of interest is not strictly positive. If the estimator works for all fields $I(\nu, \hat{\mathbf{s}})$, then that includes the subset of such fields that are restricted to be positive.